Estimation of effective intestinal membrane permeability considering bile micelle solubilisation

Kiyohiko Sugano *

Global Research & Development, Sandwich Laboratories, Research Formulation, Pfizer Inc., CT13 9NJ, Sandwich, Kent, UK

ABSTRACT

In this study, the calculation method of effective intestinal membrane permeability (P_{eff}) for bile micelle solubilised drugs was investigated. The intestinal membrane permeation is the tandem process of unstirred water layer (UWL, superimposes to the mucus layer) and epithelial cell membrane permeation. In most cases of lipophilic compounds, UWL permeation is the rate-limiting step. Four scenarios of UWL permeation were investigated: (A) only free drug permeates the UWL by self-diffusion, (B) both free drug and micelle bound drug permeate through the UWL by self-diffusion, (C) water convection carries the drug in addition to (B), and (D) both free drug and bile micelle bound drug permeate through the UWL by self-diffusion with the diffusion coefficient of the free monomer. Using danazol as a model drug, the simulation results of the four scenarios were compared with the observed fraction of a dose absorbed (Fa%) in fasted and fed state humans (fasted: 11–25%, fed: 44–72%). Scenario (A) largely underestimated the fraction of a dose absorbed (2% and 2% for fasted and fed, respectively). Scenarios (B) and (C) predicted the Fa% appropriately (B: 8% and 43%, C: 17% and 60%). Scenario (D) overestimated the Fa% (62% and 99%). The relationship between octanol–water partition coefficient and P_{eff} was also investigated.

© 2008 Elsevier B.V. All rights reserved.

1. Introduction

Computational oral absorption simulation is expected to be an effective tool in drug discovery and development (Jones et al., 2006; Kuentz et al., 2006; Parrott and Lave, 2002; Takano et al., 2006; Sugano et al., 2007). In the current drug discovery paradigm, the number of low solubility compounds is increasing (Lipinski, 2000; Sugano et al., 2007). Therefore, oral absorption simulation for low solubility compound is currently extensively investigated. In the case of low solubility compounds, bile micelle solubilisation in the small intestine plays an important role for oral absorption.

However, there are discrepancies between the theories and the experimental observations for bile micelle solubilised drugs: (1) in several reports of oral absorption simulation for low solubility drugs, the total concentration in bile micelle media (free drug + micelle bound drug) and membrane permeability of free monomer (e.g., obtained from Caco-2 cell assay) were simultaneously used for simulation, resulting in appropriate in vivo prediction (corresponding to scenario D described below) (Jones et al., 2006; Takano et al., 2006). However, in theory, when the permeability value of free monomer is used, the concentration of free

molecule (free fraction) should be used instead of the solubility in bile micelle media. (2) It is well known that many low solubility compounds undergo the positive food effect, due to the increase of solubility by bile micelles (Gu et al., 2007). However, if only free monomer molecules are available for permeation, there should be no positive food effect, since solubilisation by bile micelles does not increase the free monomer concentration. Therefore, it is of great interest to investigate the reason for these discrepancies.

The intestinal membrane permeation is the tandem process of unstirred water layer (UWL) and epithelial cellular membrane permeation (Fig. 1). The unstirred water layer superimposes to the mucus layer. In most cases of lipophilic compounds (the octanol–water distribution coefficient ($\log D_{oct} > 2$–3), cellular membrane permeation is very rapid. Therefore, UWL permeation would be the rate-limiting step for lipophilic compounds (Avdeef et al., 2007; Fagerholm and Lennernaes, 1995; Lennernaes, 2007a; Obata et al., 2005; Sugano et al., 2003; Youdim et al., 2003).

Previously, it was suggested that bile micelles can permeate through the UWL by self-diffusion, and therefore, bile micelles work as the carrier of a compound (Amidon et al., 1982; Li et al., 1996). Micelles from self-emulsifying drug delivery system (SEDDS) formulation were also suggested to permeate through the UWL (Araya et al., 2006; Porter et al., 2007). In addition, it is well known that nano-scale particles (ca <500 nm) can permeate through the mucus layer (Norris and Sinko, 1997; Sanders et al., 2000). The effect of

* Tel.: +44 1304 644338.
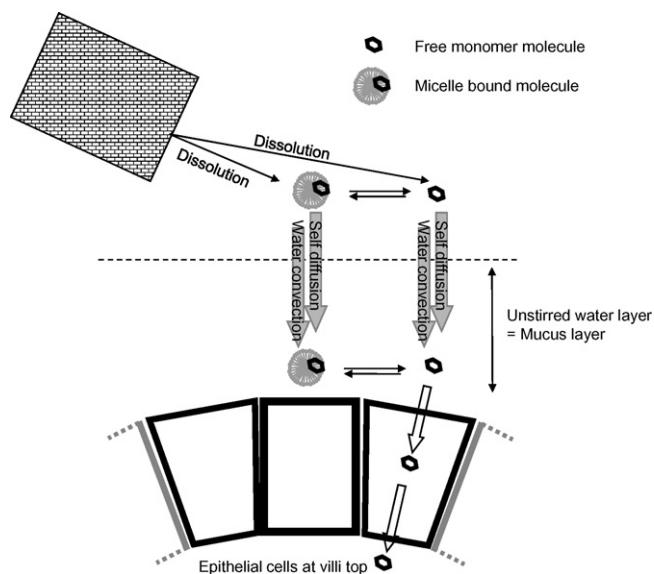*E-mail address:* Kiyohiko.Sugano@pfizer.com.

Fig. 1. Schematic presentation of intestinal membrane permeation. Both free monomer molecule and micelle bound molecule can permeate the unstirred water layer. The equilibrium between the monomer and micelle bound molecule are rapid and free monomer fraction permeate the epithelial membrane.

water convection on UWL permeability has been suggested in addition to self-diffusion (Nilsson et al., 1994; Pappenheimer, 2001). However, UWL permeation of a bile micelle bound drug has not been considered in oral absorption simulation.

In this study, four scenarios of UWL permeation were considered (Fig. 1).

(A) Only free monomer molecule (free fraction) permeates the UWL by self-diffusion.
(B) Both free monomer molecules and bile micelle bound molecules permeate across the UWL by self-diffusion.
(C) (B) plus convection accompanying water absorption (water convection).
(D) Both free drug and bile micelle bound drug permeate through the UWL by self-diffusion with the diffusion coefficient of the free monomer.

The predicted values of the fraction of a dose absorbed (Fa%) by the four scenarios were compared with the clinical oral absorption data for danazol, a typical low solubility compound.

2. Theory

2.1. P_{eff} equation

In the case of a low solubility compound, solubility in the intestinal fluid is often increased by bile micelles. In this study, the effective concentration for permeation in the intestinal fluid (C_{eff}) is defined as the sum of the concentrations of free molecules and the bile micelle bound molecules (Sugano et al., 2007). The absorption rate (dX_{abs}/dt) can be described as

$$\frac{dX_{abs}}{dt} = SA_{si} P_{eff} C_{eff} = \frac{SA_{si}}{V_{si}} P_{eff} C_{eff} V_{si} = k_a X_{eff} \tag{1}$$

where SA_{si} is the effective surface area of the small intestine, P_{eff} is the effective intestinal membrane permeability, V_{si} is the effective volume of the intestinal fluid, k_a is the absorption rate constant ($=SA_{si}/V_{si} \times P_{eff}$), and X_{eff} is the drug amount which is available for permeation ($C_{eff} \times V_{si}$).

The human small intestine has a fold and villi structure. The UWL is on the top of the villi structure. Therefore, P_{eff} can be described as

$$\frac{1}{P_{eff}} = \left(\frac{1}{P_{ep,eff}} + \frac{1}{P_{UWL,eff}} \right) \frac{1}{FE}$$

$$= \left(\frac{1}{Acc\, VE\, f_{mono} P_{ep}} + \frac{1}{P_{UWL,eff}} \right) \frac{1}{FE} \tag{2}$$

where $P_{ep,eff}$ is the effective epithelial cellular membrane permeability ($=Acc \times VE \times f_{mono} \times P_{ep}$), P_{ep} is the epithelial cellular membrane permeability of free monomer, f_{mono} is the fraction of free monomer, $P_{UWL,eff}$ is the effective UWL permeability, Acc is the accessibility to the villi surface, VE is the surface expansion by villi structure (VE = 10 in humans) (DeSesso and Jacobson, 2001; Oliver et al., 1998), and FE is the surface expansion by fold structure (FE = 3 in humans) (DeSesso and Jacobson, 2001). Acc depends on P_{ep}, f_{mono}, the effective diffusion coefficient in the UWL ($D_{UWL,eff}$) and the permeability by water convection (P_{WC}). Acc was calculated according to the reference (Oliver et al., 1998). In this equation, it was assumed that only free monomer molecules can permeate the epithelial membrane.

$P_{UWL,eff}$ of the above four scenarios A–D can be represented as Eqs. (3)–(6), respectively:

$$P_{UWL,eff} = \frac{f_{mono} D_{UWL,mono}}{h_{eff}} \tag{3}$$

$$P_{UWL,eff} = \frac{D_{UWL,eff}}{h_{eff}} = \frac{1}{h_{eff}}(f_{mono} D_{UWL,mono} + f_{mic} D_{UWL,mic}) \tag{4}$$

$$P_{UWL,eff} = \frac{D_{UWL,eff}}{h_{eff}} + P_{WC,eff} = \frac{1}{h_{eff}}(f_{mono} D_{UWL,mono} + f_{mic} D_{UWL,mic})$$
$$+ (f_{mono} P_{WC,mono} + f_{mic} P_{WC,mic}) \tag{5}$$

$$P_{UWL,eff} = \frac{D_{UWL,mono}}{h_{eff}} \tag{6}$$

where h_{eff} is the effective thickness of the UWL, f_{mic} is the fraction of micelle bound molecule ($1 - f_{mono}$), $D_{UWL,mono}$ and $D_{UWL,mic}$ are the diffusion coefficients of free monomer and micelle bound molecules in the UWL, respectively, and $P_{WC,mono}$ and $P_{WC,mic}$ are the permeability of free monomer and micelle bound molecules by water convection, respectively.

2.1.1. Calculation of intrinsic epithelial membrane permeability

P_{ep} for undissociated molecular species was estimated from the relationship between to the octanol–water partition coefficient (P_{oct}) and the Caco-2 intrinsic membrane permeability of undissociated molecular species ($P_{caco,int}$) as

$$P_{ep} = P_{caco,int} = A P_{oct}{}^B \tag{7}$$

where A and B are 2.36×10^{-6} and 1.10 respectively (Fig. 2) (Avdeef et al., 2005). P_{ep} of danazol (log P_{oct} = 4.2) (Glomme et al., 2006) was calculated to be 0.098 cm/s.

2.1.2. Calculation of free monomer fraction

The f_{mono} can be calculated as

$$f_{mono} = \frac{S_{buffer}}{S_{micelles}} \tag{8}$$

where $S_{micelles}$ is the solubility in biorelevant media with bile micelles and S_{buffer} is the solubility in the buffer without bile micelles. The measured solubility values in the fasted state and fed simulated intestinal fluid (FaSSIF and FeSSIF, respectively) were used for simulation (Galia et al., 1998; Vertzoni et al., 2004). FaSSIF
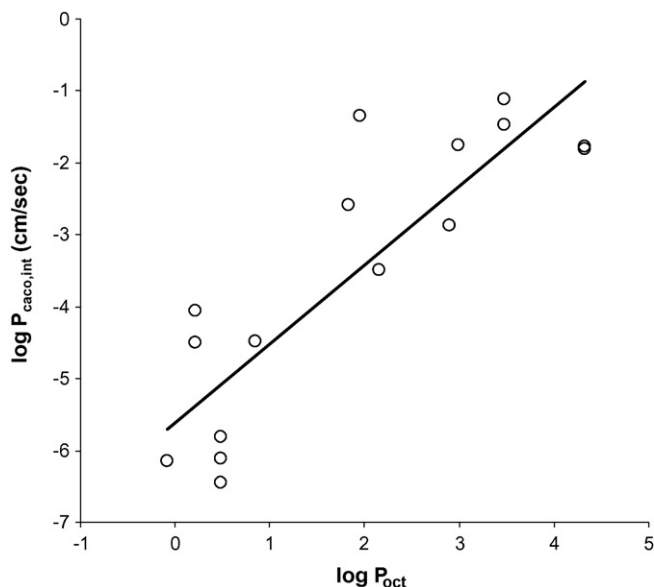
Fig. 2. Log P_{oct} vs Caco-2 intrinsic permeability. Data obtained from Avdeef et al. (2005) $P_{caco,int}$ is the permeability of undissociated species in Caco-2 assay $P_{caco,int} = 2.36 \times 10^{-6} \times P_{oct}^{1.1}$.

and FeSSIF consist of taurocholic acid (TC) and egg lecithin (EL): TC/EL = 3 mM/0.75 mM for FaSSIF and TC/EL = 15 mM/3.75 mM for FeSSIF. The solubility values of danazol in buffer, FaSSIF and FeSSIF are 0.00021, 0.018 and 0.047 mg/mL, respectively (Okazaki et al., 2008). The f_{mono} was calculated to be 0.012 and 0.0045 in FaSSIF and FeSSIF, respectively. Previously, Glomme et al. (2006) proposed an equation to estimate $S_{micelles}$ of TC/EL micelles from log P_{oct} for undissociable compounds

$$S_{micelles} = S_{int} \left(1 + \frac{C_{bile}}{C_{water}} 10^{\log K_{bm}}\right) \tag{9}$$

$$\log K_{bm} = 0.75 \log P_{oct} + 2.27 \tag{10}$$

where S_{int} is the intrinsic solubility, K_{bm} is the bile micelle–water partition coefficient, C_{bile} is the concentration of taurocholic acid, and C_{water} is the concentration of water (55.55 M).

2.1.3. Diffusion coefficients of free monomer and bile micelles in UWL

D_{mono} of danazol was set to be 8×10^{-6} cm²/s (Okazaki et al., 2008). The diffusion coefficients of bile micelles in FaSSIF and FeSSIF were 0.12×10^{-6} cm²/s and 1.05×10^{-6} cm²/s, respectively (the bile micelle diameters were 54.4 nm and 6.3 nm, respectively) (Okazaki et al., 2008). It was reported that the mucus layer only slightly affected the diffusion coefficient of bile micelles at TC > 10–20 mM range, whereas mucus layer increases the diffusion coefficient more than 3-fold at TC < 10–20 mM range (Li et al., 1996). Therefore, for fasted state, 0.36×10^{-6} cm²/s was used, whereas the same value (1.05×10^{-6} cm²/s) as in the buffer was used for fed state (Li et al., 1996).

2.1.4. Thickness of the unstirred water layer

The apparent thickness of the UWL (h_{app}) has been calculated from P_{eff} and $D_{UWL,eff}$ for UWL limited permeation compounds using Eq. (2) assuming $P_{ep,eff} \gg P_{UWL,eff}$ and FE = 1, as

$$h_{app} = \frac{D_{UWL,eff}}{P_{eff}} \tag{11}$$

Lennernas et al. reported h_{app} to be ca. 100 μm in humans (Fagerholm and Lennernaes, 1995; Lennernaes, 2007a). However,

Eq. (11) does not consider the fold structure. If the fold structure is considered, the mucus thickness on the villi is ca. 300 μm. This value is in good agreement with the thickness of the mucus layer obtained by direct measurements (170–480 μm in the small intestine) (Atuma et al., 2001). In this study, 300 μm was used as h_{eff}.

2.1.5. Estimation of UWL permeability by water convection

Lennernas et al. reported that the water absorption rate was 1.3 ± 3.0, 2.6 ± 2.2, and 3.7 ± 3.5 mL/h/cm for each experiment (Fagerholm et al., 1999; Lennernaes et al., 1994; Nilsson et al., 1994). Lambert et al. (1997) reported the water absorption was 3.3 mL/h/cm) in the jejunum and much higher in the duodenum. On average, the water absorption is 2.7 mL/h/cm/GI length in humans, which corresponds to 0.69×10^{-4} cm/s (based on the intestinal tube radius (r_{GI}) of 1.75 cm, 1 cm GI length = 11.0 cm²). This value is based on the smooth tube surface area same as P_{eff} calculation. Considering the 3-fold expansion by the fold structure, $P_{WC,eff} = 0.23 \times 10^{-4}$ cm/s was used for UWL permeability calculation in this study. This value was used for the permeability by water convection for both monomer and micelle bound drug ($P_{WC,eff} = P_{WC,mono} = P_{WC,mic}$).

3. Oral absorption simulation

A compartment transit absorption model consisting of nine compartments (1 for the stomach, 7 for the small intestine, and 1 for the colon) was used for oral absorption simulation (Haruta et al., 1998; Jinno et al., 2006; Yu and Amidon, 1999). Dissolution and absorption in the stomach and colon were neglected in the same way as in previous reports (Jones et al., 2006; Kuentz et al., 2006; Parrott and Lave, 2002; Takano et al., 2006). Dissolution in the small intestine was simulated by the Nernst–Brunner equation (NBE) as previously reported (Okazaki et al., 2008). Log-normal distribution of particle size was assumed with $d_{50} = 4.46$ μm (Sunesen et al., 2005b) and standard deviation of 0.693 log unit. Spherical particle shape was assumed. The dissolution of danazol was reported to be simulated appropriately by this method (Okazaki et al., 2008).

Transfer of particles was simulated by assigning 100 virtual particles to each particle size bin. In this way, the transfer of particles and the reduction of particle radius by dissolution could be simultaneously taken into account. First-order kinetics with $T_{1/2} = 10$ min and $T_{1/2} = 30$ min were used for stomach emptying in fasted state and fed state, respectively (Sugito et al., 1990). The total intestinal transit time was set to be 3.5 h ($T_{1/2} = 21$ min for each small intestine compartment) (Yu, 1999).

P_{eff} was converted to absorption rate constant (k_a) as

$$k_a = \frac{SA_{si}}{V_{si}} P_{eff} = SVR\, P_{eff} = \frac{2DF}{r_{GI}} P_{eff} \tag{12}$$

where SVR is the surface/volume ratio ($=SA_{si}/V_{si}$), and DF is the degree of flatness of the intestinal tube (DF = 1 for a cylindrical tube) (Chiou, 1994). SVR can be obtained from the relationship between Fa% and P_{eff} using low permeability-high solubility drugs, assuming that colonic absorption is negligible (Fagerholm et al., 1997; Sutton et al., 2006) and the mean transit time through the small intestine (T_{si}) is 3.5 h. Fa% can be expressed as Eq. (13) by assuming the seven-compartment model (Yu et al., 1996)

$$Fa\% = \left(1 - \left(1 + \frac{k_a T_{si}}{7}\right)^{-7}\right) 100$$

$$= \left(1 - \left(1 + \frac{SVR\, P_{eff} T_{si}}{7}\right)^{-7}\right) 100 \tag{13}$$

Eq. (13) was fitted to the Fa–P_{eff} relationship previously reported (Lennernaes, 2007a). SVR for human was obtained to be 2.2 and this value was used in this study.

For the intestinal fluid volume (V_{si}), 600 mL (8.6 mL/kg) has been reported for oral absorption simulation simulation (Takano et al., 2006; Yu, 1999). On the other hand, Schiller et al. (2005) reported that the total volume of water pocket measured by water-sensitive magnetic resonance imaging is 105 mL in the human small intestine. However, this value might not be the real total volume available along the intestine, since only the free volume in the water pocket was counted (Lennernaes, 2007b). Biopharmaceutical classification system employs 250 mL (Yu et al., 2002). The same volume was also used to simulate the dose-dependent absorption of Gabapentin by active transport (Madan et al., 2005). Other reports also suggest smaller fluid volume than 600 mL (Macheras et al., 1990; Masaoka et al., 2006). In this study, the intestinal fluid volume was assumed to be 250 mL (36 mL in each compartment).

Numeric integration was performed by 4th Runge–Kutta method with integration interval of 0.5 min. The simulation programme was developed in-house utilizing Microsoft Excel Visual Basic Application (Microsoft Corporation, Redmont, WA).

4. Results and discussion

4.1. Fa% prediction for danazol

The observed Fa% values of danazol in humans were obtained as follows (Table 1). Sunesen et al. (2005b) reported that the absolute bioavailability (BA%$_{abs}$) of a danazol capsule (d_{50} = 4.46 μm) was 11% in fasted state, and the relative bioavailability against fed state (BA%$_{rel}$ = AUC(fasted)/AUC(fed)) was 25%. Since BA%$_{abs}$ < Fa% < BA%$_{rel}$, it is appropriate to estimate Fa% = 11–25% (The BA%$_{rel}$ was calculated from the AUCs of oral administration. Therefore, the first pass effect was cancelled out. However, oral absorption in the fed state could be incomplete and the AUC for complete absorption could be larger. Therefore, Fa% is smaller than BA%$_{rel}$.). In another report from Charman et al. (1993) BA%$_{rel}$ of a capsule dosed in the fasted state against the emulsion formation in the fed state was 23%. If i.v. data from Sunesen et al. was used, BA%$_{abs}$ was 19%. Therefore, it would be appropriate to estimate Fa%$_{solid}$ = 19–23%. Overall, Fa% of a danazol capsule in fasted state humans would be 11–25%. Fa% in the fed stated was estimated in the same way to be 44–72%. The Fa% of emulsion formation in the fed state was assumed to be 100%, because of the non-existence of dose independency in this formulation.

Table 1
PK data of danazol in humans[a].

Formulation	Dose (mg)	Fasted/fed	AUC (ng/(h^{-1} mL^{-1}))	BA%$_{abs}$	BA%$_{rel}$
Solid[a]	100	Fasted	120 ± 60	11 14[b], 25[c]	
Solid[a]	100	Fed	469 ± 164	44	–
i.v.[a]	50		531 ± 104		
Solid[d]	100	Fasted	204 ± 125	19[e]	23[b]
Solid[d]	100	Fed	639 ± 259	60[e]	72[b]
Emulsion[d]	100	Fasted	779 ± 189	73[e]	88[b]
Emulsion[d, f]	100	Fed	844 ± 194	83[e]	–
Emulsion[d]	50	Fed	296 ± 78	56[e]	–
Emulsion[d, f]	100	Fed	695 ± 171	65[e]	–
Emulsion[d]	200	Fed	1415 ± 303	67[e]	–

[a] Data from Sunesen et al. (2005b).
[b] Relative BA% against AUC of the emulsion formulation in the fed data.
[c] Relative BA% against AUC of the fed data of the same study.
[d] Data from Charman et al. (1993).
[e] Calculated based on the i.v. data from Sunesen et al. (2005b).
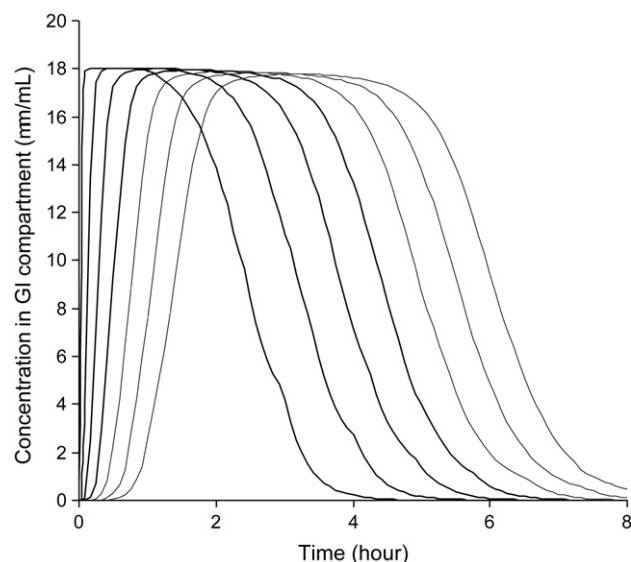[f] Different cohort.

Fig. 3. Predicted concentration–time profile in the small intestine for danazol at 100 mg dose in fasted state humans. The numbers in the figure correspond to each small intestinal compartment (from left to right, compartment 1–7, proximal to distal, respectively).

The P_{ep} value of danazol, 0.098 cm/s, was obtained from the relationship between Caco-2 intrinsic permeability and log P_{oct} (Fig. 2). In an in vitro system using plate wells, the apparent permeability is usually less than 50×10^{-6} cm/s since it is interfered with by the thick UWL. In an in vitro system, this UWL can be ca. 2000–4000 μm depending on the agitation conditions (Avdeef et al., 2004; Fujikawa et al., 2007; Youdim et al., 2003). In the case of dissociable compounds, the intrinsic permeability can be obtained from the pH-permeability profile and pK_a data (Avdeef et al., 2005; Sugano, 2007). However, in the case of undissociable compounds such as danazol, this method can no be applied. Therefore, P_{ep} value for danazol was estimated by Eq. (7) using log P_{oct}. Even though this was an estimated value, the estimation error had little effect on the prediction results, since the predicted $P_{ep,eff}$ of danazol is much higher than UWL permeability which is less than 10×10^{-4} cm/s. The insensitivity of Fa% (less than 3% difference) at the P_{ep} value of >0.01 cm/s was confirmed (data not shown).

Log-normal distribution of particle size was assumed since only the d_{50} data was available. However, in the case of solubility limited absorption, such as in the case of danazol capsules, the estimation error of the dissolution rate has little effect on the Fa% prediction (Sugano et al., 2007; Takano et al., 2006; Yu, 1999).

The SVR value obtained from the P_{eff}–Fa% relationship was 2.2. This value is higher than the theoretical value for a cylindrical tube ($2/r_{GI}$ = 1.3, r_{GI} = 1.5 cm in humans) (Yu, 1999), suggesting that the intestinal tube is rather flat (DF = 1.7) (Chiou, 1994).

In all simulation conditions, the calculated concentration in the small intestine reached the saturated solubility (Fig. 3). Although the mean T_{si} was set to be 3.5 h, the predicted concentration in the 6th and 7th compartments remained to be the saturated solubility until ca. 5 h, because a portion of the undissolved particles remain in the small intestine (Sugito et al., 1990) and maintain the saturated solubility.
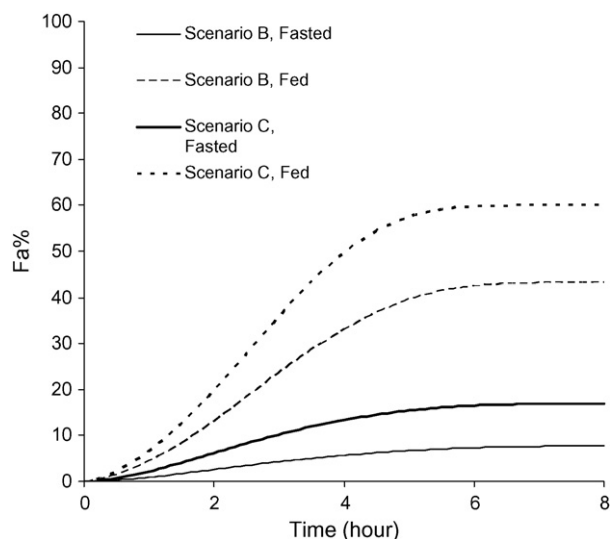
Predicted P_{eff} and Fa% in scenarios A–D are shown in Table 2. Scenario A largely underestimated Fa% values. On the other hand, scenarios B and C resulted in good prediction. Scenario D largely overestimated Fa%.

The Fa%–time profiles predicted by scenarios B and C were also in good agreement with the previous results of Sunesen et al. (2005a) (Fig. 4).

Table 2
Simulation results for Fa% of danazol in humans (dose = 100 mg).

Fasted/fed	Scenario	Predicted P_{eff} ($\times 10^{-4}$ cm/s)	Predicted Fa%
Fasted	A (Eq. (3))	0.07	2
	B (Eq. (4))	0.44	8
	C (Eq. (5))	1.1	17
	D (Eq. (6))	8.0	62
Fed	A (Eq. (3))	0.04	2
	B (Eq. (4))	1.0	43
	C (Eq. (5))	1.6	60
	D (Eq. (6))	8.0	99

Fig. 4. Fa%–time profile predicted by scenarios B and C for danazol at 100 mg dose in fasted and fed state humans.

Recently, Persson et al. (2008) measured the P_{eff} of danazol dissolved in bile media using an intestinal perfusion model in pigs. Iso-osmotic solution was used to neglect water absorption. Therefore, the experimental condition corresponded to scenario B. The predicted P_{eff} value by scenario B (=0.44 × 10⁻⁴ cm/s) in this study was in good agreement with the experimental result of ca. 0.4 × 10⁻⁴ cm/s in Persson's study.
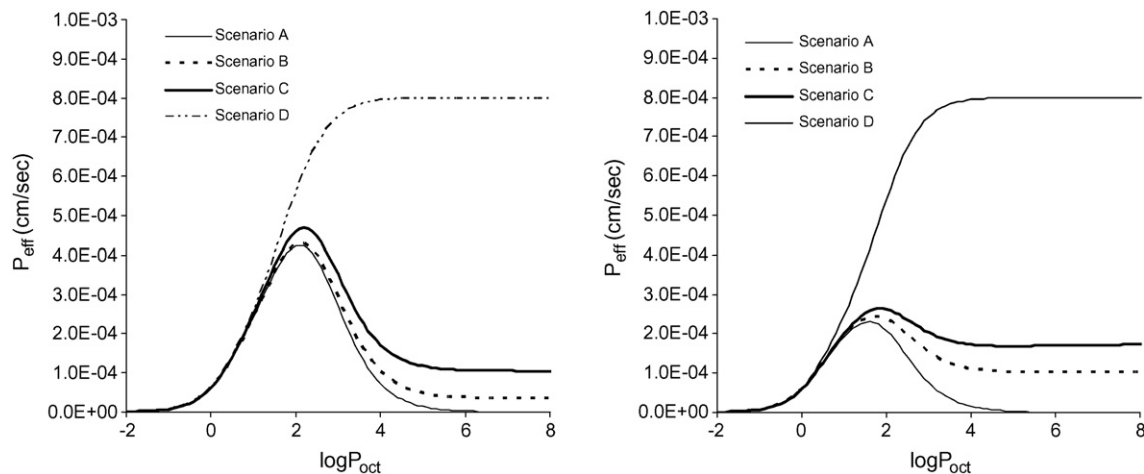
Even considering some uncertainty in input of physiological and compound parameters, scenarios B and C were suggested to be more appropriate compared to scenarios A and D based on the large prediction error (Table 2). This was in good agreement with the previously proposed mechanism (Amidon et al., 1982; Araya et al., 2006; Li et al., 1996; Porter et al., 2007). However, more accurate estimation for the intestinal fluid volume, the UWL thickness, the diffusion coefficient of bile micelles in the mucus layer, the flatness of the intestinal tube, and the solubility in the intestinal fluid would be required to draw a conclusion about scenarios B and C from a simulation predictability aspect. In this study, danazol was used as a model drug, since all clinical pharmacokinetic data (solid dosage, p.o. solution and i.v.), particle size, solubility and physicochemical properties were available in the literature. The same conclusion was obtained for felodipine and danazol in dogs (manuscript under preparation).

Takano et al. previously employed scenario D for fasted state, and over estimation was also found for most low solubility compounds (e.g., for danazol, predicted Fa = 40%). However, the extent of overestimation in their study is less than that in this study (Predicted Fa = 62%). In their simulation, they assumed a single compartment for the small intestine and at 4 h all particles exited the small intestine at once, where as in this study it was suggested that a portion of particles remained in the small intestine for longer time than 4 h (Fig. 3).

4.2. $Log P_{oct} - P_{eff}$ profile

Since both P_{ep} and K_{bm} can be predicted by $\log P_{oct}$, $\log P_{oct} - P_{eff}$ profile can be drawn (Fig. 5). This figure is not precisely quantitative due to the rough estimation of P_{ep} and K_{bm} by $\log P_{oct}$. For example, f_{mono} of danazol calculated by Eqs. (9) and (10) were 0.066 and 0.014 for FaSSIF and FeSSIF, respectively (experimental values were 0.012 and 0.0045). However, it would be beneficial to understand a general trend with a logarithmic scale. In $\log P_{oct} < 2$ range, as $\log P_{oct}$ increased, P_{eff} also increased. In this $\log P_{oct}$ region, the epithelial membrane permeation would be the rate-limiting step. If bile micelle binding is not significant (corresponds to scenario D), P_{eff} increases up to ca. 8×10^{-4} cm/s at which the UWL limits permeability. However, if the bile micelle binding is significant as Eq. (10) predicts, as lipophilicity increased to over 2, P_{eff} decreases due to the increase of micelle binding (decrease of f_{mono}). Micelle binding decreases both $P_{UWL,eff}$ and $P_{ep,eff}$ by reducing the effective diffusion coefficient and the free monomer fraction, respectively. P_{eff} value achieved a constant value of bile micelle permeation at $\log P_{oct} > 4$, because the power of the micelle partition equation (Eq.

Fig. 5. $\log P_{oct}$ vs P_{eff} predicted by scenarios A–D for humans. (A) Fasted state, (B) fed state. TC = 3 mM and TC = 15 mM were used for the fasted state and fed state, respectively. P_{ep} and K_{bm} were calculated from $\log P_{oct}$ by Eqs. (7) and (10), respectively. P_{eff} was calculated from P_{ep} and K_{bm} by Eqs. (2)–(6). $D_{UWL,mono}$ was set to 8×10^{-6} cm²/s.

(10), 0.75) is lower than that of the epithelial membrane permeation equation (Eq. (7), 1.10). In $\log P_{oct} < 4$ range, predicted P_{eff} in the fed state is lower than that in the fasted state, due to smaller f_{mono} in the fed state. On the other hand, in $\log P_{oct} > 4$ range, predicted P_{eff} in the fed state is higher than that in the fasted state, due to the higher diffusion coefficient of bile micelles in the fed state (Okazaki et al., 2008; Sugano et al., 2007).

5. Conclusion

In this study, a mathematical equation for P_{eff} was introduced to simulate oral absorption from bile micelles. Estimation of UWL permeability is the key for appropriate simulation. A similar approach can be applied to the UWL permeation of nano-scale formulations, such as SEDDS (Porter et al., 2007) and nano-milled particles (Jinno et al., 2006; Liversidge and Cundy, 1995). Application of the methodology for nano-milled particles is under investigation.

Acknowledgements

References

Amidon, G.E., Higuchi, W.I., Ho, N.F.H., 1982. Theoretical and experimental studies of transport of micelle-solubilized solutes. J. Pharm. Sci. 71, 77–84.
Araya, H., Tomita, M., Hayashi, M., 2006. The novel formulation design of self-emulsifying drug delivery systems (SEDDS) type O/W microemulsion III: the permeation mechanism of a poorly water soluble drug entrapped O/W microemulsion in rat isolated intestinal membrane by the ussing chamber method. Drug Metab. Pharmacokinet. 21, 45–53.
Atuma, C., Strugala, V., Allen, A., Holm, L., 2001. The adherent gastrointestinal mucus gel layer: thickness and physical state in vivo. Am. J. Physiol. 280, G922–G929.
Avdeef, A., Artursson, P., Neuhoff, S., Lazorova, L., Grasjo, J., Tavelin, S., 2005. Caco-2 permeability of weakly basic drugs predicted with the Double-Sink PAMPA pKfluxa method. Eur. J. Pharm. Sci. 24, 333–349.
Avdeef, A., Bendels, S., Di, L., Faller, B., Kansy, M., Sugano, K., Yamauchi, Y., 2007. Parallel artificial membrane permeability assay (PAMPA)-critical factors for better predictions of absorption. J. Pharm. Sci. 96, 2893–2909.
Avdeef, A., Nielsen, P.E., Tsinman, O., 2004. PAMPA—a drug absorption in vitro model. 11. Matching the in vivo unstirred water layer thickness by individual-well stirring in microtitre plates. Eur. J. Pharm. Sci. 22, 365–374.
Charman, W.N., Rogge, M.C., Boddy, A.W., Berger, B.M., 1993. Effect of food and a monoglyceride emulsion formulation on danazol bioavailability. J. Clin. Pharmacol. 33, 381–386.
Chiou, W.L., 1994. Effect of 'unstirred' water layer in the intestine on the rate and extent of absorption after oral administration. Biopharm. Drug Dispos. 15, 709–717.
DeSesso, J.M., Jacobson, C.F., 2001. Anatomical and physiological parameters affecting gastrointestinal absorption in humans and rats. Food Chem. Toxicol. 39, 209–228.
Fagerholm, U., Lennernaes, H., 1995. Experimental estimation of the effective unstirred water layer thickness in the human jejunum, and its importance in oral drug absorption. Eur. J. Pharm. Sci. 3, 247–253.
Fagerholm, U., Lindahl, A., Lennernas, H., 1997. Regional intestinal permeability in rats of compounds with different physicochemical properties and transport mechanisms. J. Pharm. Pharmacol. 49, 687–690.
Fagerholm, U., Nilsson, D., Knutson, L., Lennernas, H., 1999. Jejunal permeability in humans in vivo and rats in situ: investigation of molecular size selectivity and solvent drag. Acta Physiol. Scand. 165, 315–324.
Fujikawa, M., Nakao, K., Shimizu, R., Akamatsu, M., 2007. QSAR study on permeability of hydrophobic compounds with artificial membranes. Bioorgan. Med. Chem. 15, 3756–3767.
Galia, E., Nicolaides, E., Horter, D., Lobenberg, R., Reppas, C., Dressman, J.B., 1998. Evaluation of various dissolution media for predicting in vivo performance of class I and II drugs. Pharm. Res. 15, 698–705.
Glomme, A., März, J., Dressman, J., 2006. Predicting the intestinal solubility of poorly soluble drugs. In: Testa, B., Krämer, S., Wunderli-Allenspach, H., Folkers, G. (Eds.), Pharmacokinetic Profiling in Drug Research. Wiley–VCH, Zurich, pp. 259–280.
Gu, C.-H., Li, H., Levons, J., Lentz, K., Gandhi, R.B., Raghavan, K., Smith, R.L., 2007. Predicting effect of food on extent of drug absorption based on physicochemical properties. Pharm. Res. 24, 1118–1130.
Haruta, S., Iwasaki, N., Ogawara, K.-i., Higaki, K., Kimura, T., 1998. Absorption behavior of orally administered drugs in rats treated with propantheline. J. Pharm. Sci. 87, 1081–1085.

Jinno, J.-I., Kamada, N., Miyake, M., Yamada, K., Mukai, T., Odomi, M., Toguchi, H., Liversidge, G.G., Higaki, K., Kimura, T., 2006. Effect of particle size reduction on dissolution and oral absorption of a poorly water-soluble drug, cilostazol, in beagle dogs. J. Control. Release 111, 56–64.
Jones, H.M., Parrott, N., Ohlenbusch, G., Lave, T., 2006. Predicting pharmacokinetic food effects using biorelevant solubility media and physiologically based modelling. Clin. Pharmacokinet. 45, 1213–1226.
Kuentz, M., Nick, S., Parrott, N., Roethlisberger, D., 2006. A strategy for preclinical formulation development using GastroPlus (TM) as pharmacokinetic simulation tool and a statistical screening design applied to a dog study. Eur. J. Pharm. Sci. 27, 91–99.
Lambert, G.P., Chang, R.T., Xia, T., Summers, R.W., Gisolfi, C.V., 1997. Absorption from different intestinal segments during exercise. J. Appl. Physiol. 83, 204–212.
Lennernaes, H., 2007a. Intestinal permeability and its relevance for absorption and elimination. Xenobiotica 37, 1015–1051.
Lennernaes, H., 2007b. Modeling gastrointestinal drug absorption requires more in vivo biopharmaceutical data: experience from in vivo dissolution and permeability studies in humans. Curr. Drug Metab. 8, 645–657.
Lennernaes, H., Ahrenstedt, O., Ungell, A.-L., 1994. Intestinal drug absorption during induced net water absorption in man; a mechanistic study using antipyrine, atenolol and enalaprilat. Br. J. Clin. Pharmacol. 37, 589–596.
Li, C.-Y., Zimmerman, C.L., Wiedmann, T.S., 1996. Diffusivity of bile salt/phospholipid aggregates in mucin. Pharm. Res. 13, 535–541.
Lipinski, C.A., 2000. Drug-like properties and the causes of poor solubility and poor permeability. J. Pharmacol. Toxicol. Methods 44, 235–249.
Liversidge, G.G., Cundy, K.C., 1995. Particle size reduction for improvement of oral bioavailability of hydrophobic drugs. I. Absolute oral bioavailability of nanocrystalline danazol in beagle dogs. Int. J. Pharm. 125, 91–97.
Macheras, P., Reppas, C., Dressman, J.B., 1990. Estimate of volume/flow ratio of gastrointestinal (GI) fluids in humans using pharmacokinetic data. Pharm. Res. 7, 518–522.
Madan, J., Chawla, G., Arora, V., Malik, R., Bansal, A.K., 2005. Unbiased membrane permeability parameters for gabapentin using boundary layer approach. AAPS J. 7, E224–E230.
Masaoka, Y., Tanaka, Y., Kataoka, M., Sakuma, S., Yamashita, S., 2006. Site of drug absorption after oral administration: assessment of membrane permeability and luminal concentration of drugs in each segment of gastrointestinal tract. Eur. J. Pharm. Sci. 29, 240–250.
Nilsson, D., Fagerholm, U., Lennernas, H., 1994. The influence of net water absorption on the permeability of antipyrine and levodopa in the human jejunum. Pharm. Res. 11, 1540–1544.
Norris, D.A., Sinko, P.J., 1997. Effect of size, surface charge, and hydrophobicity on the translocation of polystyrene microspheres through gastrointestinal mucin. J. Appl. Polymer Sci. 63, 1481–1492.
Obata, K., Sugano, K., Saitoh, R., Higashida, A., Nabuchi, Y., Machida, M., Aso, Y., 2005. Prediction of oral drug absorption in humans by theoretical passive absorption model. Int. J. Pharm. 293, 183–192.
Okazaki, A., Mano, T., Sugano, K., 2008. Theoretical dissolution model of polydisperse drug particles in biorelevant media. J. Pharm. Sci. 97, 1843–1852.
Oliver, R.E., Jones, A.F., Rowland, M., 1998. What surface of the intestinal epithelium is effectively available to permeating drugs? J. Pharm. Sci. 87, 634–639.
Pappenheimer, J.R., 2001. Role of pre-epithelial "unstirred" layers in absorption of nutrients from the human jejunum. J. Membr. Biol. 179, 185–204.
Parrott, N., Lave, T., 2002. Prediction of intestinal absorption: comparative assessment of GASTROPLUS and IDEA. Eur. J. Pharm. Sci. 17, 51–61.
Persson, E.M., Nordgren, A., Forsell, P., Knutson, L., Oehgren, C., Forssen, S., Lennernaes, H., Abrahamsson, B., 2008. Improved understanding of the effect of food on drug absorption and bioavailability for lipophilic compounds using an intestinal pig perfusion model. Eur. J. Pharm. Sci. 34, 22–29.
Porter, C.J.H., Trevaskis, N.L., Charman, W.N., 2007. Lipids and lipid-based formulations: optimizing the oral delivery of lipophilic drugs. Nat. Rev. Drug Discov. 6, 231–248.
Sanders, N.N., De Smedt, S.C., Demeester, J., 2000. The physical properties of biogels and their permeability for macromolecular drugs and colloidal drug carriers. J. Pharm. Sci. 89, 835–849.
Schiller, C., Frohlich, C.P., Giessmann, T., Siegmund, W., Monnikes, H., Hosten, N., Weitschies, W., 2005. Intestinal fluid volumes and transit of dosage forms as assessed by magnetic resonance imaging. Aliment. Pharmacol Therapeut. 22, 971–979.
Sugano, K., 2007. Artificial membrane technologies to assess transfer and permeation of drugs in drug discovery. In: Testa, B., van de Waterbeemd, H. (Eds.), Comprehensive Medicinal Chemistry II, vol. 5, ADME-Tox Approach. Elsevier, Oxford, pp. 453–487.
Sugano, K., Nabuchi, Y., Machida, M., Aso, Y., 2003. Prediction of human intestinal permeability using artificial membrane permeability. Int. J. Pharm. 257, 245–251.
Sugano, K., Okazaki, A., Sugimoto, S., Tavornvipas, S., Omura, A., Mano, T., 2007. Solubility and dissolution profile assessment in drug discovery. Drug Metab. Pharmacokinet. 22, 225–254.
Sugito, K., Ogata, H., Goto, H., Noguchi, M., Kogure, T., Takano, M., Maruyama, Y., Sasaki, Y., 1990. Gastrointestinal transit of non-disintegrating solid formulations in humans. Int. J. Pharm. 60, 89–97.

Sunesen, V.H., Pedersen, B.L., Kristensen, H.G., Mullertz, A., 2005a. In vivo in vitro correlations for a poorly soluble drug, danazol, using the flow-through dissolution method with biorelevant dissolution media. Eur. J. Pharm. Sci. 24, 305–313.

Sunesen, V.H., Vedelsdal, R., Kristensen, H.G., Christrup, L., Muellertz, A., 2005b. Effect of liquid volume and food intake on the absolute bioavailability of danazol, a poorly soluble drug. Eur. J. Pharm. Sci. 24, 297–303.

Sutton, S.C., Evans, L.A., Fortner, J.H., McCarthy, J.M., Sweeney, K., 2006. Dog colonoscopy model for predicting human colon absorption. Pharm. Res. 23, 1554–1563.

Takano, R., Sugano, K., Higashida, A., Hayashi, Y., Machida, M., Aso, Y., Yamashita, S., 2006. Oral absorption of poorly water-soluble drugs: computer simulation of fraction absorbed in humans from a miniscale dissolution test. Pharm. Res. 23, 1144–1156.

Vertzoni, M., Fotaki, N., Kostewicz, E., Stippler, E., Leuner, C., Nicolaides, E., Dressman, J., Reppas, C., 2004. Dissolution media simulating the intralumenal composi-tion of the small intestine: physiological issues and practical aspects. J. Pharm. Pharmacol. 56, 453–462.

Youdim, K.A., Avdeef, A., Abbott, N.J., 2003. In vitro trans-monolayer permeability calculations: often forgotten assumptions. Drug Disc. Today 8, 997–1003.

Yu, L.X., 1999. An integrated model for determining causes of poor oral drug absorption. Pharm. Res. 16, 1883–1887.

Yu, L.X., Amidon, G.L., 1999. A compartmental absorption and transit model for estimating oral drug absorption. Int. J. Pharm. 186, 119–125.

Yu, L.X., Amidon, G.L., Polli, J.E., Zhao, H., Mehta, M.U., Conner, D.P., Shah, V.P., Lesko, L.J., Chen, M.-L., Lee, et al., 2002. Biopharmaceutics classification system: the scientific basis for biowaiver extensions. Pharm. Res. 19, 921–925.

Yu, L.X., Lipka, E., Crison, J.R., Amidon, G.L., 1996. Transport approaches to the bio-pharmaceutical design of oral drug delivery systems: prediction of intestinal absorption. Adv. Drug Deliv. Rev. 19, 359–376.